

Effects of roasting temperature and duration on color and flavor of a sesame oligosaccharide-protein complex in a Maillard reaction model

Qing Guo, Shuai Xu, Hua-Min Liu^{*}, Ming-Wei Liu, Chen-Xu Wang, Zhao Qin, Xue-De Wang

College of Food Science and Engineering & Institute of Special Oilseed Processing and Technology, Henan University of Technology, Zhengzhou 450001, China

ARTICLE INFO

Keywords:

Maillard model
Oligosaccharides
Sesame protein isolate
Color
Volatile compounds

ABSTRACT

In this work, sesame oligosaccharides (SOL) and sesame protein isolate (SPI) were isolated from dehulled sesame meal, combined and then tested as a sesame model system, to investigate the effects of roasting temperature and duration on color and flavor. The results demonstrated that SOL was more easily degraded than SPI; specifically, SOL and SPI gradually degraded at 100 °C and 150 °C, respectively. FT-IR analysis showed that characteristic bonds existing in the roasted samples were somewhat destroyed. Galactose, fructose, lysine, cysteine, and arginine showed great reduction and played an important role in color variation and flavor compound formation according to monosaccharide and amino acid analysis. Total color difference (ΔE) and browning intensity increased with roasting temperature and roasting duration. The types and concentrations of volatile flavor compounds were significantly increased, particularly heterocyclics (14.1 %–34.4 %) and phenols (28.4 %–32.4 %), corresponding to 0.3 % and 8.9 % of the unroasted samples.

Introduction

Sesame oil extracted from roasted seeds is very popular with consumers due to its attractive color, taste, and distinctive aroma (Yin et al., 2021). According to previous studies, the color and aroma of sesame oil are attributed to the Maillard reaction, lipid oxidation, and thermal degradation of macromolecules such as polysaccharides and protein during roasting sesame seeds (Berk, Hamzalioglu, & Gokmen, 2019; Goncuoglu Tas & Gokmen, 2017). Many investigations have demonstrated that the thermal degradation of macromolecules and lipid oxidation provides abundant precursors for the Maillard reaction (Li et al., 2021; Ye et al., 2022). Therefore, the Maillard reaction potentially plays a key role in producing the color and flavor of sesame oil.

Roasting is a common operation in food processing, and temperature and duration are two very important factors influencing the texture, color, and flavor of roasted food (Zhang et al., 2022). Roasting can induce the Maillard reaction, which readily happens between amino compounds and reducing sugars, producing aromatic compounds, antioxidant species, and colors (Shakoor, Zhang, Xie, & Yang, 2022). In addition to abundant lipids in sesame seeds, protein and carbohydrates are the main components. Protein is one of the most important macromolecules in food, which has been confirmed to be closely associated with flavor formation (Zhang, Kang, Zhang, & Lorenzo, 2021).

Oligosaccharides are a class of water-soluble sugars that are abundant and widely distributed in nature; they commonly consist of 2–10 monosaccharides connected by α - and β - glycosidic linkages (Liu, Xie, Gu, Luo, & Li, 2022; Xiong et al., 2021). Water-soluble sugars generally play key roles in flavor formation during food processing; for example, they produce furfural and pyrones which give food what consumers recognize as a caramel flavor (Li, Shi, Li, Luo, & Li, 2022). Moreover, in plant foods, particularly fruits, there is a close relationship between flavor quality and water-soluble sugar content (Liu et al., 2011; Yang et al., 2021b). While much research has been done, the specific effects of sesame oligosaccharides (SOL) and sesame protein isolate (SPI) on color and flavor in roasting seeds have not been investigated.

Various Maillard models are widely used to investigate the contribution of specific substances to color variation and volatile flavor compound formation under different thermal treatments. For instance, Xu et al. (2021) used a peptide-xylose Maillard model to explore the mechanism of volatile compound formation in bovine bone protein. They found that taste-active peptides can produce unique flavor compounds in the absence of xylose with roasting treatment. Lotfy et al. (2021) studied the effect of pH on color and flavor compounds using a quinoa protein hydrolysate-xylose Maillard model. They concluded that pH had a great influence on the types of volatile compounds produced. Ma et al. (2022) constructed a glucose-glycine Maillard model reaction

^{*} Corresponding author.

E-mail address: liuhuamin5108@163.com (H.-M. Liu).

to investigate the formation of vinylpyrazines, which is the characteristic flavor compound in hot-processed foods. They found that the carbon atoms on the pyrazine ring of vinylpyrazines came from glucose and the vinyl group was derived from both glucose and glycine. It can be seen that the Maillard model is a convenient and feasible method to investigate how thermal treatments produce substances that influence the color and flavor of foods.

Therefore, a Maillard model reaction was established in this work, to study the interactions of SOL and SPI in producing color and flavor changes under different roasting conditions, thus exploring the contributions of SOL and SPI to the distinctive aroma of sesame oil. The chemical compositions of the unroasted and roasted SOL-SPI complex were assessed, the degree of the Maillard reaction was determined, and the volatile compounds produced were characterized. This work provides some information on color and flavor development in the process of roasting sesame seeds.

Materials and methods

Materials

The sesame seeds (Zhuzhi-22) used in this experiment were provided by the Henan Academy of Agricultural Sciences (Zhengzhou, China), and were refrigerated at 4 °C for the next step. Sesame kernels were manually obtained by dried decortication. The sesame kernels were defatted firstly using a cold-press method (50 MPa, 40 min), then further defatted with petroleum. The sesame meal was crushed to obtain the 60-mesh powder using a high-speed grinder (FW-100, Guangming instrument, China), then washed twice with 95 % ethanol at room temperature for 2 h to remove pigments, free sugars, and free amino acids. What remained was the alcohol-insoluble substance (AIS). AIS was freeze-dried, then used for the oligosaccharide and protein isolate extractions. All chemicals used in this experiment were provided by Shanghai Macklin Biochemical Technology Co., Ltd. (Shanghai, China) and they were of analytical grade.

Extraction of sesame oligosaccharides (SOL)

SOL was extracted from AIS based on a method described in a previous study with some modifications (Guo, Zhao, Li, Miao, & Zheng, 2019). Briefly, 100 g of AIS was added to 2000 mL of 30 % ethanol solution and stirred at 50 °C for 2 h, then centrifuged (4800 rpm, 15 min). The supernatant was concentrated to approximately 200 mL, then three volumes of 95 % ethanol (v/v) were mixed with concentrates, followed by continuous stirring at 25 °C for 1 h. The solution was refrigerated at 4 °C for 2 h, then centrifuged again (4800 rpm, 15 min). Subsequently, the supernatant was concentrated to approximately 200 mL and then freeze-dried to obtain sesame oligosaccharides.

Extraction of sesame protein isolate (SPI)

SPI was obtained using a method described in a previous report (Zhong et al., 2019). Briefly, 100 g of AIS was mixed with deionized water (1:20, w/v); the pH was adjusted to 10.0 using 1 mol/L sodium hydroxide. The mixture was stirred at 50 °C for 1.5 h, then centrifuged (4800 rpm, 15 min). Subsequently, the pH was adjusted to 4.5 using 1 mol/L hydrochloric acid, then centrifuged again (4800 rpm, 10 min). The precipitate was washed three times with deionized water, then freeze-dried and named SPI.

Preparation of SOL-SPI samples

Equal parts of SOL and SPI (1:1, w/w) were mixed, then added to deionized water at a ratio of 1:25 (w/v), continuously stirred at room temperature for 1.5 h, then freeze-fried. This constituted the lyophilized sample. Subsequently, portions of this were roasted at 160/180 °C for 5/

10 min (i.e., four different combinations of conditions). The unroasted sample was named UOP. The samples roasted at 160 °C for 5 min and 10 min were called ROP-1 and ROP-2, respectively. The samples roasted at 180 °C for 5 min and 10 min were named ROP-3 and ROP-4, respectively. In total, five samples were prepared for this experiment, i.e., UOP, ROP-1, ROP-2, ROP-3, and ROP-4.

Yields and chemical analysis of SOL and SPI

The yields of SOL and SPI were calculated based on the defatted sesame kernel meal (w/w). The chemical compositions of SOL and SPI were analyzed in terms of protein, moisture, and ash content according to the methods of AOCS (American Oil Chemists' Society (2017) with minor modifications. Total sugars were measured by the phenol-sulfuric acid method using D-glucose as standard (Dubois, Gilles, Hamilton, Rebers, & Smith, 1956).

Thermal gravimetric measurement

The STA 449C thermal analyzer (Netzsch, Germany) was used to measure the thermal stability of SOL and SPI. Before measurement, approximately 10 mg of SOL and SPI were dried at 100 °C for 1 h to evaporate free water, then placed in a crucible. In a nitrogen environment, the sample was heated from 45 °C to 650 °C at a rate of 10 °C/min. Thermogravimetry (TG) and differential thermogravimetry (DTG) spectra were recorded.

Fourier transform infrared (FT-IR)

FT-IR spectra of SOL, SPI, UOP, and ROP (1–4) were recorded by an IR spectrometer (Perkin Elmer Frontier, American). Approximately 5 mg of each sample was fully ground with 500 mg KBr, then pressed into a pellet for measurement. Frequency range: 4000–400 cm⁻¹; Resolution: 4 cm⁻¹.

Monosaccharide composition determination

The monosaccharide composition of the five samples was measured by a high-performance anion-exchange chromatography (HPAEC) instrument, equipped with an AS50 auto-sampler and an ICS5000 system (Thermo Fisher Scientific, USA). According to the method in our previous study (Guo et al., 2022), 5 mg of each sample was hydrolyzed with 0.125 mL of 72 wt% sulfuric acids at 25 °C for 45 min, then 1.35 mL of deionized water was added, and the mixture was heated at 105 °C for 2.5 h. Subsequently, the hydrolysates were filtered through a 0.22 μm nylon membrane, then the pH was adjusted to 7.0 using 1 mol/L hydrochloric acid. Finally, 50 μL of the resulting solution was injected into the HPAEC system. Changes in the monosaccharide compositions of the five samples were calculated using the following formula.

$$\text{Content change (\%)} = (A_0 - A_x)/A_0 \times 100\%$$

where A_0 represents the sugar content of UOP, and A_x represents the sugar content of one of the four roasted samples, i.e., ROP (1–4).

Amino acid composition determination

The amino acid composition of UOP and ROP (1–4) was assessed based on a previous method (Yang et al., 2021a). In brief, 30 mg of each sample was put into a sealed glass tube, then 10 mL of 6 mol/L hydrochloric acid and three drops of phenol were added. After nitrogen was blown over the sample for 2 min, each sample was put in an oven for 22 h at 110 °C. The hydrolysates were filtered and diluted with deionized water in a 50 mL volumetric flask. 1 mL of each solution was concentrated and evaporated to dryness, then 1 mL of deionized water was added and evaporated again. Then the dried samples were dissolved in 1

mL of citric acid solution (pH 2.2) and filtered through a 0.22 μm PES membrane (Merck, Darmstadt, Germany). The resulting solutions were identified using an S433D Automatic Amino Acid Analyzer (SYKNM, Germany). The content change in amino acid was calculated using the following formula.

$$\text{Content change (\%)} = (A_0 - A_x)/A_0 \times 100\%$$

where A_0 represents the sugar content of UOP, and A_x represents the sugar content of one of the four roasted samples, i.e., ROP (1–4).

Color measurement

The color of UOP and ROP (1–4) was measured. Briefly, approximately 1 g of each sample was put in a dish and detected by chroma-meter CR-400 (Konica Minolta, Japan). The values of L^* , a^* , b^* , and ΔE correspond to brightness, the degree of red and green (+red, –green), the degree of yellow and blue (+yellow, –blue), and the total color difference, respectively. The ΔE value was calculated by the formula below.

$$\Delta E = \sqrt{(L^* - L_0^*)^2 + (a^* - a_0^*)^2 + (b^* - b_0^*)^2}$$

where L_0^* , a_0^* , and b_0^* are color parameters of UOP.

Browning intensity determination

The browning intensity of UOP and ROP (1–4) was measured. Briefly, 10 mg of each sample was added to 30 mL deionized water, continuously stirred for 2 h at 25 °C, then centrifuged (4500 rpm, 10 min); the supernatant was collected. The absorbances of the supernatants at 294 nm and 420 nm were recorded using a UV-2401PC spectrophotometer (Shimadzu Co., Ltd., Japan). Deionized water was used as the blank control.

Identification of volatile compounds

Based on a previous report (Yuan, Peng, Zhong, Zhao, & Lin, 2021), the volatile compounds were detected using headspace solid-phase microextraction coupled with gas chromatography-mass spectrometry (HS-SPME/GC-MS). In brief, 1 g of each sample was tightly sealed in a 15 mL glass vial, containing a magnet rotor, then continuously stirred with a magnetic stirrer (60 °C, 40 min). The volatile flavor compounds were extracted with a DVB/CAR/PDMS-50/30 μm fiber (Sigma-Aldrich, Shanghai, China) at 60 °C for 30 min, then injected into the GC-MS system. The system used was an Agilent 7890B GC equipped with an Agilent 5977A mass spectrometry detector (Agilent Co., Ltd., Palo Alto, USA). An HP-5MS column (30 m \times 0.25 mm \times 0.25 μm , Agilent) was used to separate volatile compounds under helium (99.99%) with a flow rate of 1.8 mL/min. The heating protocol: temperature kept at 40 °C for 3.5 min; increased to 230 °C (4 °C/min) and held for 8 min; then increased to 250 °C (10 °C/min) and held for 10 min. The HP-5MS column was used in electron mode, with an electron energy of 70 eV, scanning over a range of 30–550 m/z at 2.0 scan/s. The temperatures of the MS source and the quadrupole were kept at 230 °C and 150 °C, respectively. The National Institute of Standards and Technology mass spectral library (NIST17) was used to identify the volatile compounds. The relative content of volatiles was calculated by the peak area normalization method.

Statistical analysis

The experiments in this work were carried out at least three times. The data were subjected to one-way analysis of variance (ANOVA) using IBM SPSS statistics 21.0 software (Chicago, USA), and the values shown are the mean \pm standard deviation (SD). Duncan's multiple range test

was performed and significant differences were considered when $P < 0.05$.

Results and discussion

Chemical compositions and yields of SOL and SPI

The yields and chemical compositions of SOL and SPI are presented in the [supplementary materials Table S1](#). As seen, the yields of SOL and SPI were 10.2% and 43.1%, respectively; the total sugar content of SOL and protein content of SPI were 78.4% and 86.7%, respectively. It can be seen that SOL had more moisture than SPI, which was attributed to the lower degree of polymerization of SOL, which meant that many more hydrophilic groups were exposed to the external environment, resulting in water being easily adsorbed to its surface. The ash content of SOL and SPI were 4.6% and 1.2%, respectively; this was related to the extraction method above.

Thermal stability

The TG and DTG spectra of SOL and SPI are presented in [Fig. 1A and B](#), respectively. As can be seen, the mass loss was divided into three phases. The first phase of mass loss of SOL (<100 °C) and SPI (<150 °C) was ascribed to the evaporation of residual water in the lyophilized samples. The mass loss during this phase was below 2% because SOL and SPI had already been heated at 100 °C for 1 h to remove free water before thermogravimetry determination. The second phase was the phase of major mass loss for both SOL and SPI, corresponding to the range of 100–500 °C and 150–500 °C, respectively. Mass loss during this phase was attributed to the breakage of glycosidic bonds and peptide bonds, resulting in depolymerization and degradation of SOL and SPI (Bikaki, Shah, Muller, & Kuhnert, 2021; Long et al., 2022), which in turn provided numerous intermediate compounds for the Maillard reaction to promote color and flavor formation. The mass loss reached 50% at 333.4 °C and 348.3 °C for SOL and SPI, respectively. Temperatures exceeding 500 °C represented the third phase of mass loss, corresponding to the charring of organic substances. SOL showed higher solid residue content (36.0%) than SPI (31.7%) at 650 °C. From DTG curves, it can be seen that SOL and SPI reached their maximum degradation rates at 207.1 °C and 301.6 °C, corresponding to 5.8%/°C and 5.9%/°C, respectively. From the TG and DTG curves of SOL and SPI, it can be seen that SOL is easier to degrade than SPI, showing high reactive activity because SOL had lower Mw and a relatively simple structural configuration compared with SPI (Yang, Dai, Sun, McClements, & Xu, 2022; Zou et al., 2016). Therefore, SOL can easily participate in the Maillard reaction to promote color and flavor formation. The results of total sugar reduction as shown below also support this speculation.

FT-IR analysis

The FT-IR spectra of SOL, SPI, UOP, and ROP (1–4) are presented in [Fig. S1](#). As for SOL, its spectrum showed characteristic absorption peaks in the range of 4000–500 cm^{-1} . The absorption peak at 3432 cm^{-1} was attributed to the stretching vibration of –OH and the peak at 2926 cm^{-1} was assigned to the stretching vibration of –CH(–CH₂). The weak absorption at 1727 cm^{-1} and relatively strong absorption at 1640 cm^{-1} were caused by the esterification and non-esterification of –COOH, respectively. The peaks at 1415 cm^{-1} and 1263 cm^{-1} were related to –CH₂ bending and COO– of uronic acids, respectively (Al-Wraikat, Liu, Wu, Ali, & Li, 2022). The peaks in the range of 1000–1200 cm^{-1} were mainly related to C–O–H and C–O–C stretching vibrations (Bai, Zhou, Zhu, & Li, 2022). The absorption at 925 cm^{-1} suggested the presence of α -glycosidic bonds.

In the spectrum of SPI, the peaks at 3294 cm^{-1} and 2930 cm^{-1} were related to the stretching vibration of N–H and –CH(–CH₂), respectively. Commonly, the absorption peaks at 1630–1680 cm^{-1} , 1530–1560 cm^{-1} ,

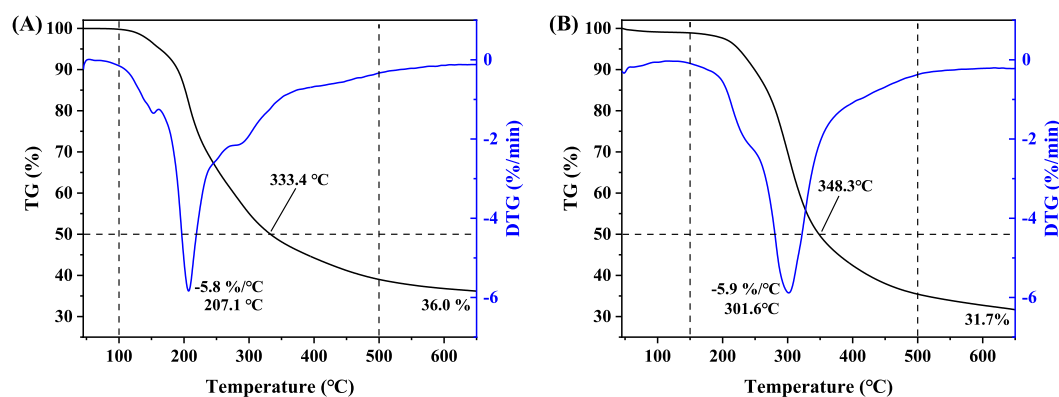


Fig. 1. Thermogravimetry (TG) and differential thermogravimetry (DTG) spectra of (A) SOL and (B) SPI. SOL, sesame oligosaccharides; SPI, sesame protein isolate.

and 1260–1420 cm^{-1} belong to amide I, amide II, and amide III, respectively (Wang, Wu, & Liu, 2017). The sharp absorption peaks at 1654 cm^{-1} and 1535 cm^{-1} were caused by the stretching vibration of C=O for amide I and the bending vibration of C–N stretching vibration for amide II. Weak absorption bands appeared at 1450 cm^{-1} and 1397 cm^{-1} due to bending stretching of N–H and stretching vibrations of C–N, respectively, for amide III (Wang et al., 2017).

The spectrum of UOP showed strong and sharp absorptions, which was similar to ROP-1, suggesting that the roasting conditions, i.e., 160 °C/5 min, could not destroy the characteristic bonds of UOP. However, as the roasting temperature and duration increased, these peaks weakened. The spectra of ROP-2, ROP-3, and ROP-4 showed weak and flat absorption peaks compared to ROP-1. This phenomenon indicated that the higher temperature and longer duration caused a deeper degree of the Maillard reaction, resulting in a darker color and many more volatile flavor compounds.

Sugar composition analysis

The sugar compositions of the unroasted and roasted samples are presented in Table 1. As can be seen, the total sugar content was 40.05, 36.27, 35.26, 33.04, and 30.63 g/100 g, corresponding to UOP, ROP-1, ROP-2, ROP-3, and ROP-4, respectively.

Table 1
Monosaccharide composition of UOP and ROP (1–4).

Monosaccharide composition (g/100 g)	Samples				
	UOP	ROP-1	ROP-2	ROP-3	ROP-4
Ara	0.24 ± 0.01 ^a	0.23 ± 0.01 ^a	0.24 ± 0.01 ^a	0.24 ± 0.02 ^a	0.24 ± 0.03 ^a
Rha	0.76 ± 0.01 ^a	0.75 ± 0.00 ^a	0.71 ± 0.00 ^b	0.69 ± 0.00 ^c	0.65 ± 0.01 ^d
Gal	13.06 ± 0.09 ^a	9.50 ± 0.12 ^b	9.18 ± 0.06 ^c	8.75 ± 0.08 ^d	8.56 ± 0.03 ^d
Glc	21.85 ± 0.02 ^a	21.72 ± 0.04 ^a	21.49 ± 0.08 ^b	20.03 ± 0.03 ^c	18.27 ± 0.08 ^d
Xyl	0.30 ± 0.01 ^a	0.29 ± 0.00 ^a	0.29 ± 0.00 ^a	0.29 ± 0.01 ^a	0.29 ± 0.01 ^a
Man	0.38 ± 0.01 ^a	0.37 ± 0.01 ^a	0.33 ± 0.00 ^b	0.33 ± 0.01 ^b	0.30 ± 0.01 ^c
Fru	3.11 ± 0.06 ^a	3.05 ± 0.06 ^a	2.68 ± 0.02 ^b	2.37 ± 0.02 ^c	2.10 ± 0.02 ^d
GalA	0.38 ± 0.01 ^a	0.37 ± 0.01 ^{ab}	0.36 ± 0.01 ^{ab}	0.35 ± 0.00 ^b	0.26 ± 0.01 ^c
Total	40.05 ± 0.04 ^a	36.27 ± 0.25 ^b	35.26 ± 0.16 ^c	33.04 ± 0.18 ^d	30.63 ± 0.17 ^e

Abbreviations: UOP, unroasted sample; ROP-1, sample roasted at 160 °C for 5 min; ROP-2, sample roasted at 160 °C for 10 min; ROP-3, sample roasted at 180 °C for 5 min; ROP-4, sample roasted at 180 °C for 10 min; Ara, arabinose; Rha, rhamnose; Gal, galactose; Glc, glucose; Xyl, xylose; Man, mannose; Fru, fructose; GalA, galacturonic acid. The different small letters in a row represent the significant difference ($P < 0.05$).

ROP-2, ROP-3, and ROP-4, respectively. The results demonstrated that increased roasting temperature and duration significantly accelerate sugar reduction due to a deeper degree of caramelization and Maillard reaction occurring. Compared to ROP-1, ROP-2 showed no obvious difference in total sugar content but ROP-3 presented a lower total sugar content, indicating that roasting temperature had a greater influence on sugar reduction than roasting duration. As for the sugar composition of UOP, glucose (21.85 g/100 g) and galactose (13.06 g/100 g) were the predominant sugars. Fructose, rhamnose, mannose, galacturonic acid, arabinose, and xylose were also detected. After roasting under different conditions, the sugar composition showed obvious variation compared to UOP as shown in Fig. 2A. Results showed a negative correlation between sugar content and strength and duration of roasting; that is, the longer a sample was roasted and/or the higher temperature it was roasted at, the fewer sugars remained after roasting. It can be seen that galactose and fructose reduced most, suggesting they were the key

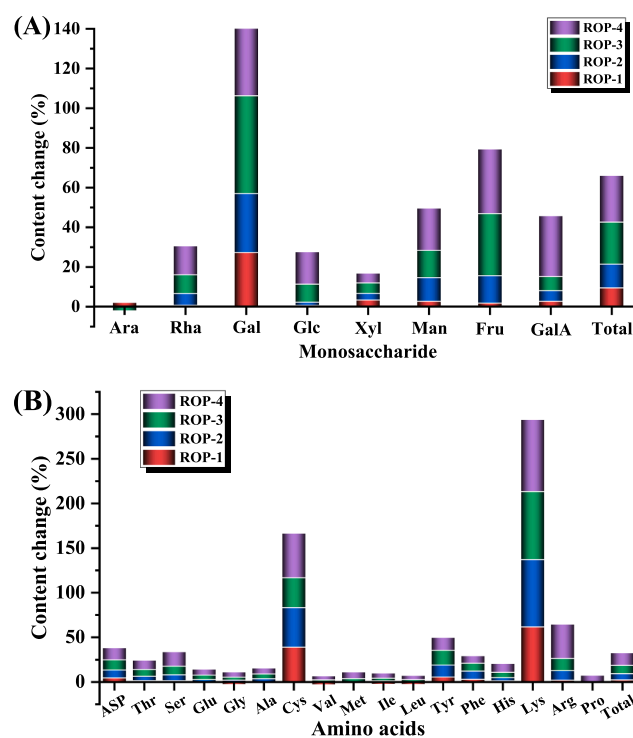


Fig. 2. Changes in (A) monosaccharide content and (B) amino acid content of the UOP and ROP (1–4). UOP, unroasted sample; ROP-1, sample roasted at 160 °C for 5 min; ROP-2, sample roasted at 160 °C for 10 min; ROP-3, sample roasted at 180 °C for 5 min; ROP-4, sample roasted at 180 °C for 10 min.

sugars that participated in the Maillard reaction. Although the reaction rate of glucose was lower than galactose and fructose, the content of glucose did decrease significantly. The results contradicted Laroque et al. (2008), who found the sugar reactivity order was xylose > arabinose > glucose \approx fructose in this sugar-hydrolysate Maillard model. The phenomenon was mainly attributed to the differences in precursor types and roasting conditions, which greatly influence the degree of thermal reactions induced by roasting, resulting in color and flavor being significantly different (Shang et al., 2019).

Amino acid composition analysis

The amino acid compositions of UOP and ROP (1–4) are shown in Table 2. As can be seen, seventeen amino acids were detected in SPI, of which glutamic acid (9.92 g/100 g), arginine (5.73 g/100 g), and aspartic acid (5.17 g/100 g) were the most abundant. Total amino acids were 50.53, 49.39, 46.96, 45.9, 43.33 g/100 g, corresponding to UOP, ROP-1, ROP-2, ROP-3, and ROP-4, respectively. It can be seen that increasing the roasting temperature and duration reduced the total amino acids. Comparing the total amino acids of ROP-1, ROP-2, and ROP-3, the total amino acids of ROP-3 decreased more than ROP-2, from which it can conclude that roasting temperature had a greater effect on the degree of Maillard reaction than duration. This conclusion is not consistent with that of Sun et al. (2022), who found roasting duration had a stronger effect on volatile compounds, presumably due to differences in materials and roasting conditions. Notably, the total amino

Table 2
Amino acid composition of UOP and ROP (1–4).

Amino Acid (g/100 g)	Samples				
	UOP	ROP-1	ROP-2	ROP-3	ROP-4
Asp	5.17 \pm 0.02 ^a	4.94 \pm 0.01 ^b	4.71 \pm 0.01 ^c	4.58 \pm 0.01 ^d	4.47 \pm 0.02 ^e
Thr	2.08 \pm 0.01 ^a	2.05 \pm 0.01 ^a	1.98 \pm 0.01 ^b	1.92 \pm 0.01 ^c	1.86 \pm 0.01 ^d
Ser	2.27 \pm 0.02 ^a	2.24 \pm 0.01 ^a	2.12 \pm 0.02 ^b	2.05 \pm 0.01 ^c	1.90 \pm 0.01 ^d
Glu	9.92 \pm 0.09 ^b	9.94 \pm 0.02 ^a	9.66 \pm 0.02 ^c	9.43 \pm 0.02 ^d	9.24 \pm 0.01 ^e
Gly	2.66 \pm 0.01 ^b	2.74 \pm 0.01 ^a	2.61 \pm 0.01 ^c	2.57 \pm 0.02 ^d	2.50 \pm 0.01 ^e
Ala	2.80 \pm 0.01 ^a	2.83 \pm 0.01 ^a	2.70 \pm 0.01 ^b	2.65 \pm 0.01 ^c	2.61 \pm 0.01 ^d
Cys	0.18 \pm 0.01 ^a	0.11 \pm 0.01 ^b	0.10 \pm 0.01 ^{bc}	0.12 \pm 0.01 ^b	0.09 \pm 0.01 ^c
Val	2.79 \pm 0.05 ^b	2.88 \pm 0.04 ^a	2.78 \pm 0.02 ^b	2.74 \pm 0.02 ^{bc}	2.66 \pm 0.03 ^c
Met	1.06 \pm 0.03 ^a	1.08 \pm 0.03 ^a	1.06 \pm 0.02 ^a	1.02 \pm 0.02 ^{ab}	0.98 \pm 0.02 ^b
Ile	2.40 \pm 0.03 ^{ab}	2.46 \pm 0.05 ^a	2.37 \pm 0.02 ^b	2.33 \pm 0.01 ^{bc}	2.26 \pm 0.02 ^c
Leu	3.80 \pm 0.03 ^b	3.91 \pm 0.03 ^a	3.80 \pm 0.03 ^b	3.70 \pm 0.03 ^c	3.62 \pm 0.02 ^d
Tyr	2.06 \pm 0.01 ^a	1.95 \pm 0.07 ^a	1.78 \pm 0.02 ^b	1.72 \pm 0.01 ^b	1.76 \pm 0.06 ^b
Phe	2.72 \pm 0.02 ^a	2.64 \pm 0.02 ^a	2.47 \pm 0.03 ^b	2.48 \pm 0.03 ^b	2.49 \pm 0.06 ^b
His	1.69 \pm 0.02 ^a	1.67 \pm 0.03 ^{ab}	1.63 \pm 0.01 ^{bc}	1.59 \pm 0.01 ^c	1.52 \pm 0.02 ^d
Lys	1.51 \pm 0.02 ^a	0.58 \pm 0.01 ^b	0.37 \pm 0.01 ^c	0.36 \pm 0.01 ^c	0.29 \pm 0.01 ^d
Arg	5.73 \pm 0.03 ^a	5.62 \pm 0.03 ^b	5.12 \pm 0.02 ^c	4.94 \pm 0.02 ^d	3.53 \pm 0.02 ^e
Pro	1.73 \pm 0.01 ^a	1.76 \pm 0.03 ^a	1.73 \pm 0.01 ^a	1.73 \pm 0.04 ^a	1.60 \pm 0.03 ^b
Total	50.53 \pm 0.43 ^a	49.39 \pm 0.31 ^b	46.96 \pm 0.33 ^c	45.90 \pm 0.32 ^d	43.33 \pm 0.40 ^e

Abbreviations: UOP, unroasted sample; ROP-1, sample roasted at 160 °C for 5 min; ROP-2, sample roasted at 160 °C for 10 min; ROP-3, sample roasted at 180 °C for 5 min; ROP-4, sample roasted at 180 °C for 10 min. The different small letters in a row represent the significant difference ($P < 0.05$).

acids decreased less than total sugars, indicating that SOL was easier to participate in the Maillard reaction than SPI because of the weak thermal stability of SOL. Generally, sugars react at a faster rate than amino compounds owing to caramelization and sugar fragmentation (Laroque et al., 2008).

The changes in amino acid content of ROP (1–4) are shown in Fig. 2B. It can be seen that all amino acids of roasted samples decreased compared with the unroasted sample but the reduction rates were different. Lysine and cysteine reduced most, followed by arginine. These three were presumably the key amino acids involved in the Maillard reaction, largely contributing to producing the attractive color and distinctive aroma. After roasting at 180 °C for 10 min, the content of lysine decreased from 1.51 g/100 g to 0.29 g/100 g, a reduction of 80.8 %, and cysteine decreased from 0.18 g/100 g to 0.09 g/100 g, a reduction of 50.0 %. Arginine as the main amino acid in SPI also showed a significant reduction. Similar results, i.e., with lysine and arginine showing significant decreases, have also been found in other studies (Ji, Liu, Shi, Wang, & Wang, 2019; Wang et al., 2021), which further confirmed the importance of these two amino acids in color and flavor formation.

Color analysis

The color variation and total color difference (ΔE) of the roasted samples are presented in Fig. 3. As shown in Fig. 3A, L^* values of all roasted samples decreased by more than 50 % after roasting at different temperatures and duration, suggesting roasting greatly decreased the brightness of samples, which was possibly related to the melanoidin derived from the Maillard reaction and caramelization reaction in roasting (Tsai et al., 2021; Zhang et al., 2022). All samples showed a significant difference ($P < 0.05$) in brightness except between ROP-2 and ROP-3. This seems to demonstrate that low roasting temperature for a long period of time can achieve similar results as high temperature for a short time. In Fig. 3B, the increase of a^* values indicated the redness of samples increased after roasting; this is presumably due to the formation of brown pigments via the Maillard reaction (Kahyaoglu & Kaya, 2006). However, the a^* values gradually decreased as the roasting temperature and duration increased, which was correlated with decreases in both L^* values and b^* values. A significant difference ($P < 0.05$) was not observed between ROP-2 and ROP-3 due to there being little difference between low roasting temperature for a long time and high roasting temperature for a short time. The b^* values of the samples are presented in Fig. 3C. As seen, ROP-1 did not differ significantly from UOP. Significant differences showed that increasing roasting temperature and duration produced many more pigments due to a deeper degree of the Maillard reaction.

Fig. 3D depicts the ΔE values of the four roasted samples. Compared with UOP, the four roasted samples showed significant differences ($P < 0.05$) except between ROP-2 and ROP-3. This phenomenon was also observed in Fig. 3A–C. Undoubtedly, among the four roasted samples, ROP-4 showed the highest total color difference because it was roasted at the highest temperature for the longest time. Therefore, roasting temperature and duration are two important factors influencing the color and flavor formation in the process of roasting sesame seeds. It is noteworthy that roasting temperature affects color differently compared with roasting duration (Sun et al., 2022).

Browning intensity

The Maillard reaction typically occurs in two phases, i.e., the early stage and the advanced stage. The early stage represents the formation of non-enzymatic intermediate compounds, while the advanced stage represents the polymerization and degradation of intermediate compounds to generate brown pigments. These brown pigments are melanoidins, which are also called advanced glycation end-products (AGEs). These early and advanced phases were measured using a UV–vis

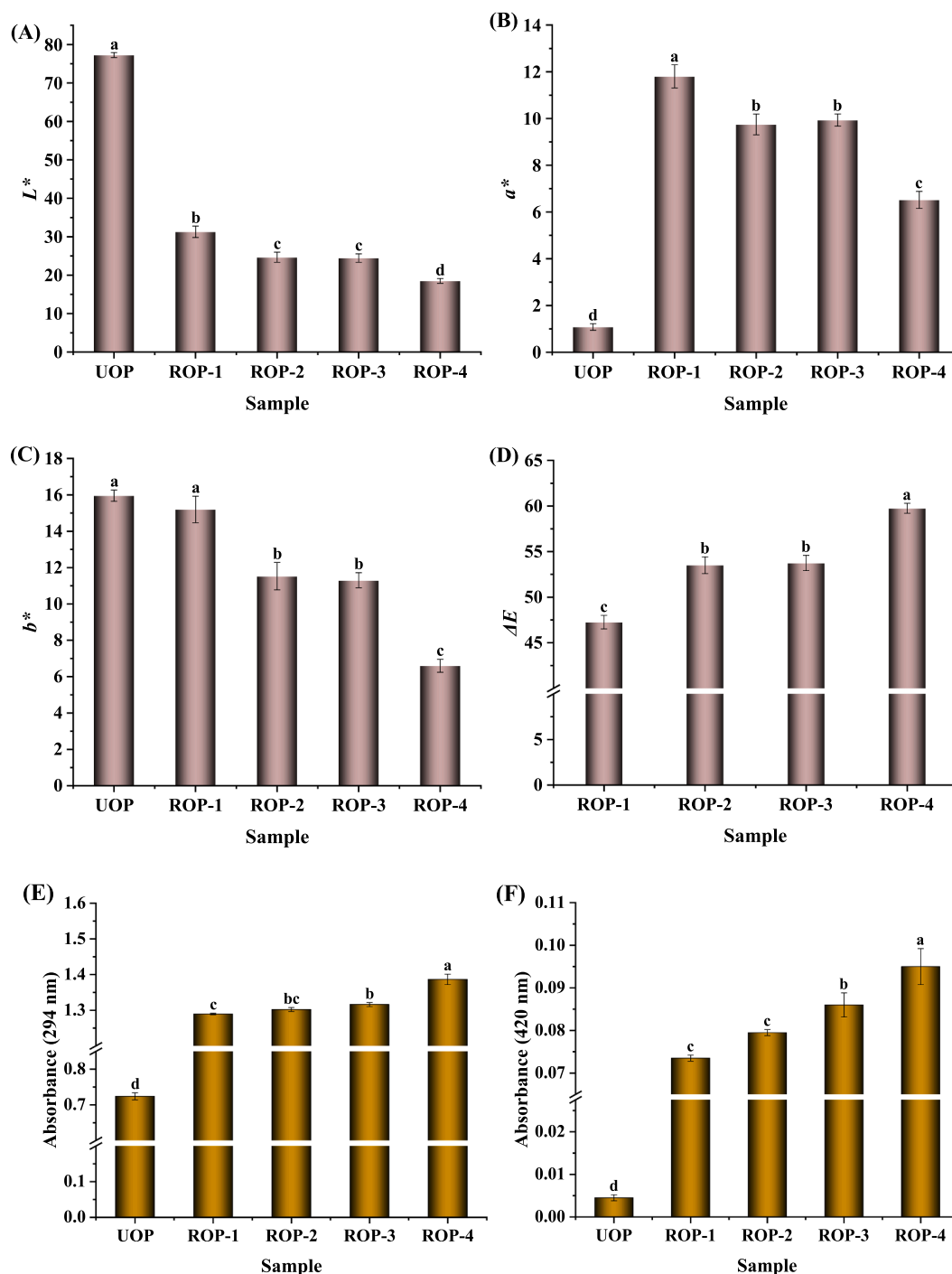


Fig. 3. Color variations and absorbance changes of UOP and ROP (1–4). (A) L^* values; (B) a^* values; (C) b^* values; (D) ΔE values; (E) absorbance at 294 nm; (F) absorbance at 420 nm. UOP, unroasted sample; ROP-1, sample roasted at 160 °C for 5 min; ROP-2, sample roasted at 160 °C for 10 min; ROP-3, sample roasted at 180 °C for 5 min; ROP-4, sample roasted at 180 °C for 10 min.

spectrophotometer at 294 nm and 420 nm, respectively (Ye et al., 2022). As can be seen in Fig. 3E, compared with UOP, the absorbances of ROP (1–4) at 294 nm showed significant increases in the range of 1.2–1.4, suggesting nearly the same amounts of browning intermediate compounds were formed in all roasted samples. However, comparing ROP-1 (160 °C for 5 min), ROP-2 (180 °C for 5 min), and ROP-3 (160 °C for 10 min), the absorbance showed no apparent increase, which demonstrated the conclusion again, that high temperature for a short time has an equivalent effect compared with low temperature for a long time. The absorbance of samples at 420 nm is shown in Fig. 3F. Compared with

UOP, the absorbances of all four roasted samples at 420 nm were significantly different ($P < 0.05$). Furthermore, they were much lower than the absorbances at 294 nm, indicating that there were more initial intermediate compounds than AGEs. However, even though they were few, these AGEs had already given a darker color to the roasted samples.

Volatile flavor compound analysis

The volatile flavor compounds of UOP and ROP (1–4) are presented in the Supplementary Data Table S2 and Fig. 4. A total of 86 volatile

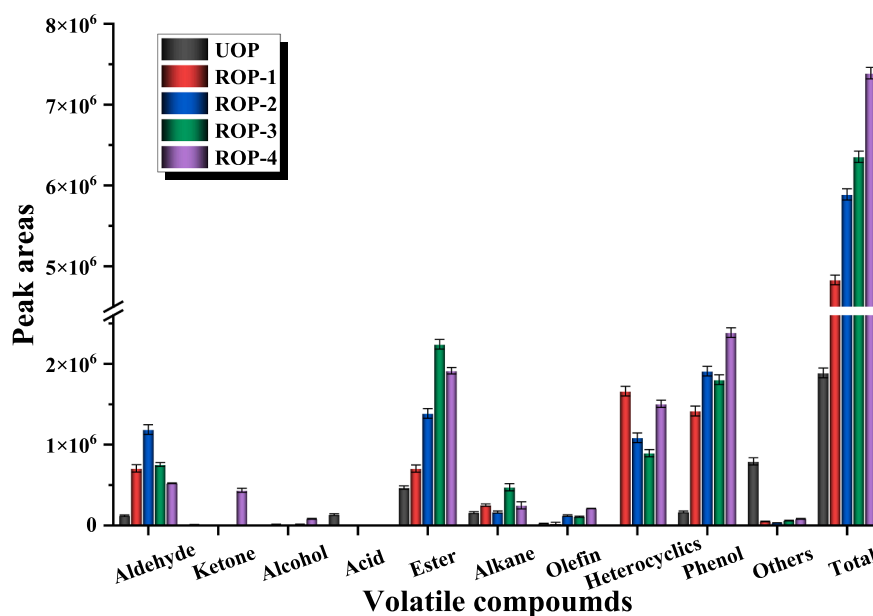


Fig. 4. Volatile compounds of the UOP and ROP (1–4). UOP, unroasted sample; ROP-1, sample roasted at 160 °C for 5 min; ROP-2, sample roasted at 160 °C for 10 min; ROP-3, sample roasted at 180 °C for 5 min; ROP-4, sample roasted at 180 °C for 10 min.

compounds were identified and classified into 9 categories as follows: aldehyde, ketone, alcohol, ester, alkane, olefin, heterocyclics, phenols, and others. The total types as well as the total content of volatile compounds increased with roasting temperature and duration. As seen in the volatile flavor compounds of UOP in Table S1, toluene was the predominant component and comprised 42.1 % of all volatiles. Toluene is one of the most important aromatic hydrocarbons; it is also abundant in the volatile compounds formed by roasting pine nuts (Adelina, Wang, Zhang, & Zhao, 2021). Small aldehydes, alkanes, and phenols were also detected in UOP. The volatile profiles of roasted samples differed significantly from UOP. Aldehydes, esters, and heterocyclics greatly increased after roasting. Heterocyclic compound content of ROP-1, ROP-2, ROP-3, and ROP-4 was 0.30 %, 34.40 %, 18.40 %, 14.1 %, and 20.4 %, respectively. As can be seen in Table S1, 2,5-dimethyl pyrazine, 3-ethyl-2,5-dimethyl-pyrazine, and 2,3-dihydro-3,5-dihydroxy-6-methyl-4H-pyran were the main nitrogen heterocyclic compounds among the volatiles. Heterocyclics such as pyrazine are regarded as the key aroma-active compounds in roasted sesame oil (Yin et al., 2021). Phenol content presented a great increase in the range of 28.4 %–32.4 % compared with UOP (8.9 %), which presumably relates to the good antioxidant activities of sesame oil (Lin et al., 2016). The results were similar to the study of Chandrasekara and Shahidi (2011), who found the total phenolic compounds, as well as antioxidant activities, increased as the roasting temperature increased during roasting whole cashew and testa, which was mainly attributed to the liberation of phenols and Maillard reaction products.

Comparing the four roasted samples, ROP-1 showed the highest content of heterocyclics, and this content decreased when the roasting temperature and duration increased. Presumably, this is because these heterocyclics convert to melanoidins under stronger roasting conditions, resulting in a darker color. The results of color analyses support this explanation. The content of aldehydes and esters firstly increased with long roasting time as seen in ROP-1 and ROP-2, but later decreased with long roasting at a higher temperature, that is in, ROP-3 and ROP-4. Similar results were also found by Adelina et al. (2021). It is probably because aldehydes and esters can be the precursors for the deeper degree of the Maillard reaction. As for the phenols in the roasted samples, there were significant differences ($P < 0.05$) between ROP-1 and ROP-2, and between ROP-3 and ROP-4, but no significant difference ($P < 0.05$)

between ROP-2 and ROP-3. This variation suggests that roasting at high temperatures for a short time has much the same effect on phenols content as roasting at low temperatures for a long time. Therefore, we speculate that stronger roasting conditions can produce much more aldehydes, esters, heterocyclics, and phenols, which play an important role in the distinctive aroma and good antioxidant activities of sesame oil (Yin et al., 2021).

Conclusion

SOL-SPI was used as a sesame Maillard model in this work to investigate the contribution of oligosaccharides and protein to color and flavor formation in roasting sesame seeds. SOL showed higher reactivity than SPI. The content of SOL and SPI significantly decreased under different roasting conditions. Higher roasting temperature and longer roasting time contribute to a deeper degree of the Maillard reaction, resulting in a darker color and many more volatile flavor compounds formed. Roasting at a high temperature for a short period (180 °C for 5 min) has much the same effect on color and flavor formation as roasting at a low temperature for a longer time (160 °C for 10 min). In the SOL-SPI model, galactose and fructose were the key compounds involved in the Maillard reaction. Lysine, cysteine, and arginine also decreased. The heterocyclic compounds and phenols showed a significant increase after roasting but their content decreased with higher roasting temperature and a longer period. Particularly, phenols produced in roasting SOL-SPI complex may relate to the good antioxidant of sesame oil and the formation mechanism needs further investigation. In summary, the interactions of oligosaccharides and protein play an important role in color and flavor formation in the process of roasting sesame seeds.

CRedit authorship contribution statement

Qing Guo: Investigation, Writing – original draft, Data curation, Methodology. **Shuai Xu:** Investigation, Software, Resources. **Hua-Min Liu:** Supervision, Writing – review & editing, Funding acquisition. **Ming-Wei Liu:** Software, Data curation. **Chen-Xu Wang:** Software, Resources. **Zhao Qin:** Supervision, Resources. **Xue-De Wang:** Project administration, Supervision.

Declaration of Competing Interest

The authors declare that they have no known competing financial interests or personal relationships that could have appeared to influence the work reported in this paper.

Data availability

Data will be made available on request.

Acknowledgments

This work was financially supported by the Natural Science Foundation of Excellent Youth for Henan (222300420038) and China Agriculture Research System of MOF and MARA (CARS-14).

Appendix A. Supplementary data

Supplementary data to this article can be found online at <https://doi.org/10.1016/j.fochx.2022.100483>.

References

- Adelina, N. M., Wang, H., Zhang, L. G., & Zhao, Y. H. (2021). Comparative analysis of volatile profiles in two grafted pine nuts by headspace-SPME/GC-MS and electronic nose as responses to different roasting conditions. *Food Research International*, *140*, Article 110026. <https://doi.org/10.1016/j.foodres.2020.110026>
- Al-Wraikat, M., Liu, Y., Wu, L. M., Ali, Z., & Li, J. K. (2022). Structural characterization of degraded Lycium barbarum L. Leaves' polysaccharide using ascorbic acid and hydrogen peroxide. *Polymers*, *14*, 1404–1419. <https://doi.org/10.3390/polym14071404>
- AOCS. (American Oil Chemists' Society, 2017). Official methods and recommended practices of the AOCS. Champaign, IL: AOCS Press.
- Bai, Y. P., Zhou, H. M., Zhu, K. R., & Li, Q. (2022). Impact of thermally induced wall breakage on the structural properties of water-soluble polysaccharides in chickpeas. *International Journal of Biological Macromolecules*, *208*, 869–882. <https://doi.org/10.1016/j.ijbiomac.2022.03.186>
- Berk, E., Hamzalioglu, A., & Gokmen, V. (2019). Investigations on the Maillard Reaction in Sesame (*Sesamum indicum* L.) Seeds Induced by Roasting. *Journal of Agriculture and Food Chemistry*, *67*, 4923–4930. <https://doi.org/10.1021/acs.jafc.9b01413>
- Bikaki, M., Shah, R., Muller, A., & Kuhnert, N. (2021). Heat induced hydrolytic cleavage of the peptide bond in dietary peptides and proteins in food processing. *Food Chemistry*, *357*, 129621. <https://doi.org/10.1016/j.foodchem.2021.129621>
- Chandrasekara, N., & Shahidi, F. (2011). Effect of roasting on phenolic content and antioxidant activities of whole cashew nuts, kernels, and testa. *Journal of Agriculture and Food Chemistry*, *59*, 5006–5014. <https://doi.org/10.1021/jf2000772>
- Dubois, M., Gilles, K. A., Hamilton, J. K., Rebers, P. A., & Smith, F. (1956). Colorimetric method for determination of sugars and related substances. *Analytical Chemistry*, *28*, 350–356. <https://doi.org/10.1021/ac60111a017>
- Goncuoglu Tas, N., & Gokmen, V. (2017). Maillard reaction and caramelization during hazelnut roasting: A multiresponse kinetic study. *Food Chemistry*, *221*, 1911–1922. <https://doi.org/10.1016/j.foodchem.2016.11.159>
- Guo, Q., Jin, L., Li, Z. A., Huang, G. W., Liu, H. M., Qin, Z., et al. (2022). Sequential extraction, preliminary characterization and functional properties of sesame (*Sesamum indicum* L.) hull polysaccharides. *LWT – Food Science and Technology*, *164*, Article 113661. <https://doi.org/10.1016/j.lwt.2022.113661>
- Guo, Z. B., Zhao, B. B., Li, H., Miao, S., & Zheng, B. D. (2019). Optimization of ultrasound-microwave synergistic extraction of prebiotic oligosaccharides from sweet potatoes (*Ipomoea batatas* L.). *Innovative Food Science and Emerging Technologies*, *54*, 51–63. <https://doi.org/10.1016/j.ifset.2019.03.009>
- Ji, J. M., Liu, Y. L., Shi, L. K., Wang, N. N., & Wang, X. D. (2019). Effect of roasting treatment on the chemical composition of sesame oil. *LWT – Food Science and Technology*, *101*, 191–200. <https://doi.org/10.1016/j.lwt.2018.11.008>
- Kahyaoglu, T., & Kaya, S. (2006). Modeling of moisture, color and texture changes in sesame seeds during the conventional roasting. *Journal of Food Engineering*, *75*, 167–177. <https://doi.org/10.1016/j.jfoodeng.2005.04.011>
- Laroque, D., Inisan, C., Berger, C., Vouland, E., Dufosse, L., & Guérard, F. (2008). Kinetic study on the Maillard reaction. Consideration of sugar reactivity. *Food Chemistry*, *111*, 1032–1042. <https://doi.org/10.1016/j.foodchem.2008.05.033>
- Li, Q., Li, X. J., Ren, Z. Y., Wang, R. J., Zhang, Y., Li, J., et al. (2021). Physicochemical properties and antioxidant activity of Maillard reaction products derived from *Dioscorea opposita* polysaccharides. *LWT – Food Science and Technology*, *149*, Article 111833. <https://doi.org/10.1016/j.lwt.2021.111833>
- Li, T. X., Shi, F. C., Li, P. H., Luo, C., & Li, D. L. (2022). A roasting method with sugar supplement to make better use of discarded tobacco leaves. *Food Science and Technology*, *42*, 36521. <https://doi.org/10.1590/fst.36521>
- Lin, J. T., Liu, S. C., Hu, C. C., Shyu, Y. S., Hsu, C. Y., & Yang, D. J. (2016). Effects of roasting temperature and duration on fatty acid composition, phenolic composition, Maillard reaction degree and antioxidant attribute of almond (*Prunus dulcis*) kernel. *Food Chemistry*, *190*, 520–528. <https://doi.org/10.1016/j.foodchem.2015.06.004>
- Liu, J. L., Chen, L., Xu, S. L., Xu, P. P., Cui, Y. D., & Chen, P. L. (2011). Effect of Aloin on the Soluble Sugars Metabolism and Flavor Quality Keeping of Gonggan. *Applied Mechanics and Materials*, *140*, 309–313. <https://doi.org/10.4028/www.scientific.net/AMM.140.309>
- Liu, K., Xie, L., Gu, H., Luo, J., & Li, X. F. (2022). Ultrasonic extraction, structural characterization, and antioxidant activity of oligosaccharides from red yeast rice. *Food Science & Nutrition*, *10*, 204–217. <https://doi.org/10.1002/fsn3.2660>
- Long, X. S., Hu, X., Xiang, H., Chen, S. J., Li, L. H., Qi, B., et al. (2022). Structural characterization and hypolipidemic activity of *Gracilaria lemaneiformis* polysaccharide and its degradation products. *Food Chem X*, *14*, Article 100314. <https://doi.org/10.1016/j.fochx.2022.100314>
- Lotfy, S. N., Saad, R., El-Massrey, K. F., & Fadel, H. H. M. (2021). Effects of pH on headspace volatiles and properties of Maillard reaction products derived from enzymatically hydrolyzed quinoa protein-xylose model system. *LWT – Food Science and Technology*, *145*, Article 111328. <https://doi.org/10.1016/j.lwt.2021.111328>
- Ma, Y. J., Wang, X. Y., Zhu, B. W., Du, M., Dong, L., Dong, X. P., et al. (2022). Model studies on the formation of 2-vinylpyrazine and 2-vinyl-6-methylpyrazine in Maillard-type reactions. *Food Chemistry*, *374*, Article 131652. <https://doi.org/10.1016/j.foodchem.2021.131652>
- Shakoor, A., Zhang, C. P., Xie, J. C., & Yang, X. L. (2022). Maillard reaction chemistry in formation of critical intermediates and flavour compounds and their antioxidant properties. *Food Chemistry*, *393*, Article 133416. <https://doi.org/10.1016/j.foodchem.2022.133416>
- Shang, Y. F., Cao, H., Wei, C. K., Thakur, K., Liao, A. M., Huang, J. H., et al. (2019). Effect of sugar types on structural and flavor properties of peony seed derived Maillard reaction products. *Journal of Food Processing and Preservation*, *44*, 14341. <https://doi.org/10.1111/jfpp.14341>
- Sun, X. L., Zhang, B., Han, J. J., Wei, C. Q., & Liu, W. Y. (2022). Effect of roasting temperature and time on volatile compounds, total tocopherols, and fatty acids of flaxseed oil. *Journal of Food Science*, *87*, 1624–1638. <https://doi.org/10.1111/1750-3841.16073>
- Tsai, Y. J., Lin, L. Y., Yang, K. M., Chiang, Y. C., Chen, M. H., & Chiang, P. Y. (2021). Effects of Roasting Sweet Potato (*Ipomoea batatas* L. Lam.): Quality, Volatile Compound Composition, and Sensory Evaluation. *Foods*, *10*, 2602–2615. <https://doi.org/10.3390/foods10112602>
- Wang, F. R., Shen, H. L., Liu, T., Yang, X., Yang, Y. L., & Guo, Y. R. (2021). Formation of pyrazines in maillard model systems: Effects of structures of lysine-containing dipeptides/tripeptides. *Foods*, *10*, 273–285. <https://doi.org/10.3390/foods10020273>
- Wang, L., Wu, M., & Liu, H. M. (2017). Emulsifying and physicochemical properties of soy hull hemicelluloses-soy protein isolate conjugates. *Carbohydrate Polymers*, *163*, 181–190. <https://doi.org/10.1016/j.carbpol.2017.01.069>
- Xiong, F., Liang, H. X., Zhang, Z. J., Mahmud, T., Chan, A. S. C., Li, X., et al. (2021). Characterization, antioxidant and antitumor activities of oligosaccharides isolated from *Evodia lepta* (Spreng) Merr. by different extraction methods. *Antioxidants*, *10*, 1842–1860. <https://doi.org/10.3390/antiox10111842>
- Xu, X. R., Yu, M. G., Raza, J., Song, H. L., Gong, L., & Pan, W. Q. (2021). Study of the mechanism of flavor compounds formed via taste-active peptides in bovine bone protein extract. *LWT – Food Science and Technology*, *137*, Article 110371. <https://doi.org/10.1016/j.lwt.2020.110371>
- Yang, K., Xu, T. R., Fu, Y. H., Cai, M., Xia, Q. L., Guan, R. F., et al. (2021a). Effects of ultrasonic pre-treatment on physicochemical properties of proteins extracted from cold-pressed sesame cake. *Food Research International*, *139*, Article 109907. <https://doi.org/10.1016/j.foodres.2020.109907>
- Yang, S. B., Meng, Z. P., Li, Y. N., Chen, R. X., Yang, Y. Z., & Zhao, Z. Y. (2021b). Evaluation of physiological characteristics, soluble sugars, organic acids and volatile compounds in “Orin” apples (*Malus domestica*) at Different Ripening Stages. *Molecules*, *26*, 807–818. <https://doi.org/10.3390/molecules26040807>
- Yang, Z. Y., Dai, L., Sun, Q. J., McClements, D. J., & Xu, X. F. (2022). Effect of molecular weight on the interfacial and emulsifying characteristics of rice glutelin hydrolysates. *Food Hydrocolloids*, *128*, Article 107560. <https://doi.org/10.1016/j.foodhyd.2022.107560>
- Ye, Y. K., Ye, S. S., Wanyan, Z. X., Ping, H., Xu, Z. X., He, S. D., et al. (2022). Producing beef flavors in hydrolyzed soybean meal-based Maillard reaction products participated with beef tallow hydrolysates. *Food Chemistry*, *378*, Article 132119. <https://doi.org/10.1016/j.foodchem.2022.132119>
- Yin, W. T., Ma, X. T., Li, S. J., Wang, X. D., Liu, H. M., & Shi, R. (2021). Comparison of key aroma-active compounds between roasted and cold-pressed sesame oils. *Food Research International*, *150*, 110794. <https://doi.org/10.1016/j.foodres.2021.110794>
- Yuan, X. L., Peng, X. J., Zhong, L. M., Zhao, C. Q., & Lin, H. B. (2021). Analysis of the characteristic flavor substances of boneless cold-eating rabbit under different preprocessing treatments. *Journal of Food Processing and Preservation*, *45*, 15812. <https://doi.org/10.1111/jfpp.15812>
- Zhang, D., Li, X. J., Zhang, Z. Y., Zhang, J., Sun, Q. C., Duan, X. L., et al. (2022). Influence of roasting on the physicochemical properties, chemical composition and antioxidant activities of peanut oil. *LWT – Food Science and Technology*, *154*, Article 112613. <https://doi.org/10.1016/j.lwt.2021.112613>
- Zhang, J., Kang, D. C., Zhang, W. G., & Lorenzo, J. M. (2021). Recent advantage of interactions of protein-flavor in foods: Perspective of theoretical models, protein

- properties and extrinsic factors. *Trends in Food Science & Technology*, 111, 405–425. <https://doi.org/10.1016/j.tifs.2021.02.060>
- Zhong, L., Ma, N., Wu, Y. L., Zhao, L. Y., Ma, G. X., Pei, F., et al. (2019). Characterization and functional evaluation of oat protein isolate-*Pleurotus ostreatus* β -glucan conjugates formed via Maillard reaction. *Food Hydrocolloids*, 87, 459–469. <https://doi.org/10.1016/j.foodhyd.2018.08.034>
- Zou, P., Yang, X., Wang, J., Li, Y. F., Yu, H. L., Zhang, Y. X., et al. (2016). Advances in characterisation and biological activities of chitosan and chitosan oligosaccharides. *Food Chemistry*, 190, 1174–1181. <https://doi.org/10.1016/j.foodchem.2015.06.076>